JOURNAL OF MATERIALS SCIENCE 22 (1987) 325–330

Microanalytical characterization of microscopic defects in NiCr-based alloys of low impurity content

J. KUNZE, H. MAI*, A. MUCHA, U. SCHLÄFER, H. WENDROCK
Zentralinstitut für Festkörperphysik und Werkstofforschung, Akademie der Wissenschaften der DDR, 8027 Dresden, DDR

The quality of thin foil components made from NiCr-based alloys can be reduced by three-dimensional defects formed during alloy preparation and rolling cycles of foil manufacturing. In particular, the appearance of microscopic holes, i.e. defects transparent to light, air or other matter, can completely prevent special applications. Thus for the optimization of foil manufacturing procedure microanalytical investigations were needed to support the decision for either a model of solely vacancy coalescence or a combined model of vacancy coalescence in the presence of second-phase inclusions and direct interaction of inclusion and roll surface. The identification of corundum particles as a major inclusion of almost all investigated transparent defects confirms that the defects are formed due to both different mechanical behaviour (of α-Al_2O_3 inclusions and NiCr-alloy) and vacancy coalescence at the appropriate phase boundary during rolling deformation.

1. Introduction

NiCr-based alloys have been used in the past as resistor materials due to their outstanding features, such as high specific electrical resistance and excellent mechanical and chemical properties. Because of the "S"-shaped anomaly of its resistance–temperature characteristics, the alloy system in the concentration range $c_{Ni} \sim 70$ to 80 wt % is of particular interest [1, 2]. It enables the manufacture of resistors having a comparatively low temperature coefficient of resistivity (TCR). The properties of importance may be optimized for different applications by additional alloying elements such as aluminium, copper, iron, silicon, titanium, cobalt and manganese in the concentration range $c_a \sim 1$ to 5 wt % [3, 4].

The efficient manufacture of high performance components from these materials requires the availability of thin foils (thickness, d_f, of some micrometres) of high perfection, e.g. an extremely low density of transparent defects. In particular, second-phase particles having a dimension of d_f and a deformation behaviour which is different from that of the surrounding matrix, can cause holes on a microscopic extent. A rough estimate shows that for the manufacture of foil resistor structures of an area $F \sim 5\,mm^2$ involving no more than one spherical inclusion of d_f size, an alloy containing precipitate contents of the order of vol. p.p.m. or below is required (ratio of the volumes of precipitate and matrix $R_p = \frac{4}{3}\pi(d_f/2)^3/d_f F$ for spherical inclusions and $d_f = 3\,\mu m$ amounts to $R_p \sim 0.52 d_f^2/F \sim 1$ vol. p.p.m.). Therefore, it must be guaranteed for the alloy that the concentrations of all the alloying elements and impurities being able to form such inclusions will not exceed their appropriate concentration limits up to which formation of coarse-dispersed particles in the matrix is prevented. Above all, the presence of oxygen, which can cause the formation of various oxides already in the melt, must be taken into consideration. Furthermore, sulphur must be noted because it can segregate in interdendritic areas or precipitate in coarse dispersion during solidification. The formation of stable nitrides or carbides in equilibrium with the diluted solution in the metal occurs preferentially hundreds of degrees Kelvin below the melting point and, due to kinetic reasons, will thus precipitate solely in a fine dispersion with an average particle size below 100 nm.

The technologies of classical metallurgy usually do not involve products of such a high purity. In particular, the initial stages of technological development of such foils are typical for a high defect density that cannot be accepted for the finished product. Therefore, the elucidation of structure and composition of these defects is an indispensable prerequisite for the recognition of their origin, for their elimination and thus for the optimization of the technological process. The major object of the paper presented here will be the demonstration of the efficiency of simultaneous application of complementary microanalytical techniques for this purpose.

2. Qualitative discussion of thermodynamic behaviour

The preparation of NiCr-based alloys for resistor applications is usually performed in such a way that the major element concentrations chosen lead to the

*Author to whom reprint requests should be addressed.

0022–2461/87 $03.00 + .12

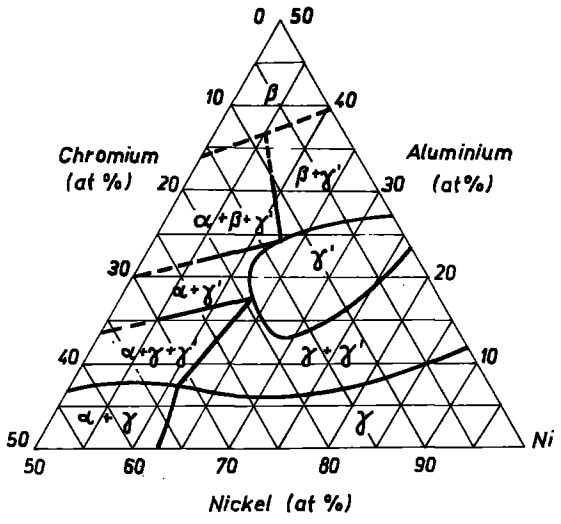

Figure 1 Ni–Cr–Al phase diagram, isothermal section at 1023 K [5].

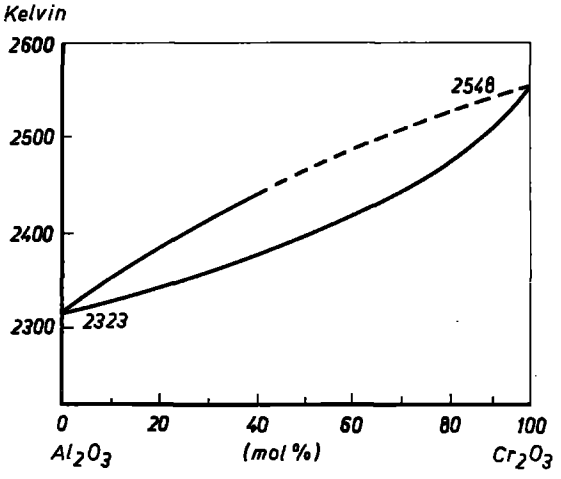

Figure 2 α-Al_2O_3–Cr_2O_3 phase diagram [11].

formation of a single-phase structure. In accordance with the NiCr binary phase diagram this is realized for $c_{Ni} \geqslant 65$ at % due to the formation of a homogeneous fcc-solid solution [5]. Before adding supplementary alloying elements this point of view must be considered. Thus the ternary NiCrAl-system having an Ni/Cr ratio $\simeq 4$ will remain a single γ-phase as long as the aluminium concentration does not exceed $c_{Al} = 5$ at % (see Fig. 1). For high aluminium concentrations only, an additional γ'-phase appears which extends its range of existence towards lower aluminium levels with decreasing temperature. Therefore, as a carefully controlled melting procedure can avoid intermetallic second phases of the major components, the resulting defects in the foils should be caused either by impurity effects or vacancy accumulation (see e.g. [6]) or a combination thereof.

Typical values of carbon, nitrogen, oxygen and sulphur impurity gross concentrations have been gathered for a representative number of ingot charges. The appropriate ranges found by hot extraction techniques are: $c_C \leqslant 20$ wt p.p.m., $c_N \leqslant 15$ wt p.p.m., $c_O \sim 10$ to 150 wt p.p.m. and $c_S \leqslant 10$ wt p.p.m. Consequently, particular attention should be paid to the behaviour of oxide formation in such systems. Similar conditions are known from the preparation of appropriate steel alloys [7].

The main parameters of alloy oxidation and consequent precipitation besides matrix composition and oxygen presence are the possible types of oxide-compounds or solid solutions (derivable from the relevant phase diagrams) and their appropriate heats of formation as well as the mobility of the atoms of different participants in the melt or solid [8]. In this respect the alloying element aluminium (as known from steel deoxidation [9]) should be of particular importance.

An oxide M_mO_n is formed according to the reaction equation

$$m[M] + n[O] = M_mO_n \qquad (1)$$

if the concentrations of the elements involved in the reaction will reach such a level that

$$\Delta^0 G = RT \ln \frac{(f_M[\%M])^m \cdot (f_O[\%O])^n}{a_{M_mO_n}} > 0 \qquad (2)$$

is obtained, where $\Delta^0 G$ is the standard value of the change in Gibbs' free energy for oxide formation from the elements M and O present in solution within the matrix, f_M, f_O are the activity coefficients of elements M and O, respectively, $a_{M_mO_n}$ is the activity of the resulting oxide, R is the universal gas constant, and T the absolute temperature (K). The activity coefficients are a measure of the extent of interactions in the melt between the various alloying component atoms M and atomic oxygen O. Their limiting values are unity as the concentrations of the alloying elements $c_i \to 0$. The activity $a_{M_mO_n} = 1$ is obtained when a pure oxide phase is formed. In the present case the formation of Al_2O_3 and Cr_2O_3 can simultaneously occur under particular conditions. According to a complete miscibility of the Al_2O_3–Cr_2O_3 system (Fig. 2) a solid solution of the composition $(Al_{1-x}Cr_x)_2O_3$ having a corundum structure is to be expected [10, 11]. The appropriate activities are characterized by the relation

$$a_{Al_2O_3} + a_{Cr_2O_3} = 1 \qquad (3)$$

For the nickel-matrix a precise prediction of the ranges of concentration and temperature where no oxide formation is observed cannot be given due to the lack of basic quantitative thermodynamic data. Thus the processes can solely be discussed using the basic data published for the iron-matrix [9]. In this case the appropriate temperature relations of the Gibbs' free energy of reaction $\Delta^0 G$ (J mol^{-1}) for oxide formation in liquid iron are [12]:

$$2[Al]_{l-Fe} + 3[O]_{l-Fe} = Al_2O_3;$$
$$\Delta^0 G = -1\,243\,000 + 395\,T \qquad (4)$$

$$2[Cr]_{l-Fe} + 3[O]_{l-Fe} = Cr_2O_3;$$
$$\Delta^0 G = -822\,900 + 360\,T \qquad (5)$$

At a temperature of $T = 1873$ K and for the approximations $f_M \sim 1, f_O \sim 1$, Equations 2, 4 and 5 yield for a composition of $c_{Cr} = 20$ wt %, $c_{Al} = 5$ wt % and $c_O = 10^{-2}$ wt % (c_{Fe} – remainder) the theoretical values $a_{Al_2O_3} = 2.7 \times 10^9$ and $a_{Cr_2O_3} = 5.6$ supposing that the total amounts of aluminium, chromium and oxygen would be present in solution. This indicates a high supersaturation in regard to Al_2O_3 formation and a merely moderate supersaturation in regard to

the formation of Cr_2O_3. The concentration of oxygen present in thermodynamic equilibrium with the pure Al_2O_3-second phase ($a_{Al_2O_3} = 1$) is then obtained from Equations 2 and 4 as $c_O \sim 6 \times 10^{-7}$ wt %. For such a low oxygen concentration from Equation 5 an equilibrium activity $a_{Cr_2O_3} = 10^{-12}$ is found.

The estimate shows that under equilibrium conditions only Al_2O_3 is formed (Cr_2O_3 content remains far below the detection limit) and the amount of oxygen remaining in solution is decreased down to some wt p.p.b. Even for low aluminium-concentrations a prevailing Al_2O_3-component should be observed in the oxide solid solution. The component of Cr_2O_3 should exceed that of Al_2O_3 only when the aluminium-concentration is decreased down to $c_{Al} \lesssim 10$ wt p.p.m. Since well-defined equilibrium conditions are usually not attained during common technological procedures in practice, a slightly increased Cr_2O_3 concentration could be supposed.

The Al_2O_3 inclusions formed, e.g. during steel deoxidation, can grow to a diameter of the order of typically 1 to 10 μm. Due to their comparatively low migration rate towards the melt surface, many of the inclusions are retained in the bulk during solidification. A qualitatively similar behaviour to that discussed above could also be supposed for the melt of an NiCr-based alloy.

Rare earth elements instead of aluminium can also be used for deoxidation purposes. In comparison to the conventional aluminium-based procedure they offer some additional advantages: higher oxygen affinity, additional formation of sulphur compounds, and formation of inclusions of lower hardness [13]. Thus at $T = 1873$ K the addition of, for example, $c_{Ce} \sim 1$ wt % to an iron melt decreases the sulphur remaining in solution to a concentration level of $c_S \sim 0.2$ wt p.p.m. However, due to the quite comparable mass densities of melt and inclusions the mechanical separation of the reaction products from the melt is still more complicated than in the case of aluminium-based deoxidation.

The discussion indicates some of the serious problems involved in the preparation of inclusion-free NiCr-based alloys. In particular the inclusions of rather high hardness remaining in the bulk after solidification should have a substantial influence on the adjacent matrix regions during plastic deformation of the ingot. Thus three-dimensional defects of various types have to be expected from

(a) vacancy coalescence at physical lattice defects in the matrix bulk (open cavities or pores empty or partially filled by dirt particles introduced during rolling procedure),

(b) vacancy coalescence i.e. cavity formation across the phase boundary matrix/second phase due to different deformation behaviour [6] (size of inclusions $d_p < d_f$), and

(c) fracture of inclusions and formation of transparent cracks within the inclusion or at matrix/inclusion phase boundary (size of inclusions $d_p \sim d_f \sim$ size of roll gap).

Therefore, microanalytical techniques are required to characterize typical defect configurations, to give a decision between the defect origins mentioned and to support the elucidation of the appropriate formation processes during foil preparation.

3. Experimental details

A number of NiCr-alloys of different aluminium content ($c_{Al} \sim <0.1$ to 2.5 wt %) have been prepared. The appropriate foils ($d_f \sim 3$ μm) have been obtained by hot and cold rolling. The quality inspection has been carried out by optical microscopy in a combined transmission/reflection mode. In general, densities of transparent micro-defects $N_d \sim 1$ to 50 per cm^2 and a lateral random defect distribution have been observed. Even for high magnification experiments in the transmission mode due to diffraction effects only rather diffuse micro-defect images could be obtained. This indicated comparable dimensions of hole diameters and illuminating light wavelength. The combination of transmission and reflection images was rendered more difficult due to a characteristic topography in the defect surroundings. Thus, on the one hand, optical structure elucidation of single defects was without result due to roughness and imaging problems. Fig. 3 shows a typical example of reflection/transmission image combination. The two bright spots indicated by arrows are hole "images". On the other hand, the defect identification by high resolution scanning electron microscopy (SEM) was quite a tedious task due to the still rather low frequency of defect appearance within the usual observation field (for a $\times$ 5000 magnification on average the probability of defect appearance within the observation field is of the order of 10^{-5} only!). Moreover a decision between transparent and nontransparent defects would usually yield ambiguous results.

Therefore, to obtain evidence of at least some statistical relevance, within cm^2 sized areas an appropriate number of typical transmitting dots have been identified in an optical low magnification mode by the transmission/reflection technique and marked by a micro-hardness pattern (see Fig. 3) for easy recognition during SEM and microanalytical investigation.

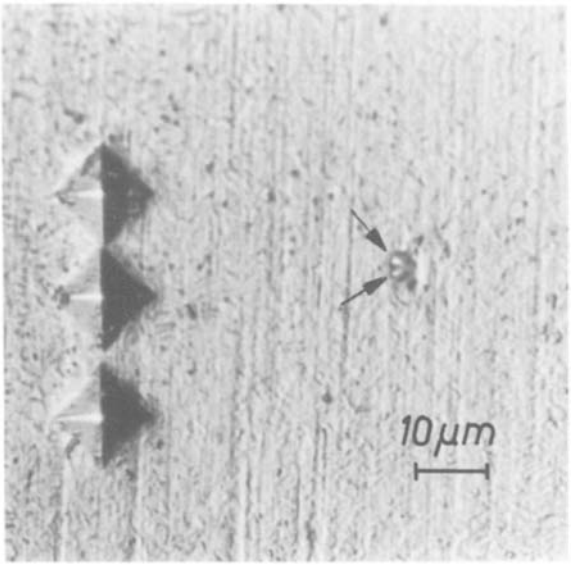

Figure 3 Optical micrograph of a typical transparent defect, combined reflection transmission imaging mode.

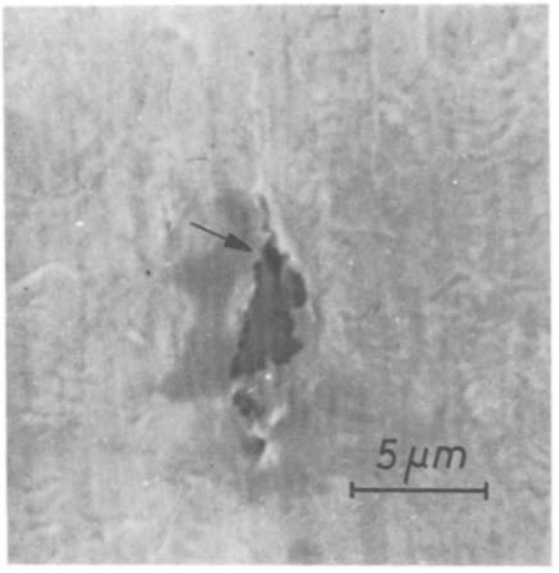

Figure 4 SEM image of transparent defect.

3.1. SEM structure elucidation

The defects detected by optical means showed under SEM investigation (JSM-S1, JEOL Tokyo, Japan) their typical configuration (Fig. 4). They are usually represented by a second-phase inclusion that involves the much smaller hole (supposed location indicated by arrow) previously discovered by optical microscopy. Whereas these holes are on average restricted to an area having a diameter, d_h, typically 0.1 to 1 μm, the second-phase particles (distinguished from the matrix by material contrast of backscattered electron, BSE, imaging) have an extent d_p typically 2 to 5 μm. This is a quite inconvenient size for elemental signal mapping by almost any microanalytical *in situ* technique. The particle is tightly enclosed by matrix substance across the major part of its circumference. Only the hole might separate the two phases from each other. Moreover cracks within the precipitates could also be assumed to be light transmitting locations. A hole without accompanying second-phase inclusion was not detectable in any case. The crystalline structure of the inclusions can be concluded from their regular habits.

The major difference observable in habit is the crack configuration, i.e. hole arrangement either between matrix and crystallite or inside the inclusion due to crystal rupture. The analytical information taken from the BSE mappings shows an almost similar mean atomic number of the inclusions within the same alloy. In comparison to the matrix, a smaller mean atomic number is always observed which indicates light element contributions.

3.2. Secondary ion mapping

The secondary ion (SI) distributions of all detectable chemical elements of all types of present inclusions and their adjacent matrix volumes have been recorded with an IMMA (Ion Microprobe Mass Analyzer, ARL Sunland, California). Owing to the extremely high elemental sensitivity of the technique and the wide range of elements that can be accepted, an elemental survey for nearly the complete Periodic Table within a concentration range from matrix contents through to lowest impurity levels is obtained.

The primary ion (PI) parameters selected for the SI-investigations were:

PI species	– $^{16}O_2^+$, $^{40}Ar^+$
PI energy	– $E(PI) = 20\,keV$
PI current	– $I(PI) = 32$ or $1\,nA$
PI beam diameter	– $d(PI) = 12$ or $3\,\mu m$

Only the elements aluminium, oxygen, chromium, nickel, sulphur, nitrogen and silicon could be detected in the various inclusions of the diverse alloys. The non-observable impurity elements possibly involved can be supposed to have concentrations in the lower p.p.m. range or even below. Thus quite pure second-phase inclusions are to be expected. Typical SI-mappings obtained from a NiCrAl-alloy are shown in Fig. 5. The intensities of the two major elements of the matrix are clearly anticorrelated to that of aluminium. In particular, no chromium content (down to the low p.p.m. range) could be detected within such inclusions of the aluminium-rich alloys. The detection of oxygen is prevented by the applied $^{16}O_2^+$ – PI. Therefore, elemental information that allows phase identification of the inclusions is to be completed by X-ray micro-analysis (EPMA).

3.3. EPMA phase identification

An SEMQ (Scanning Electron Microprobe Quantometer, ARL Sunland, California) has been used for

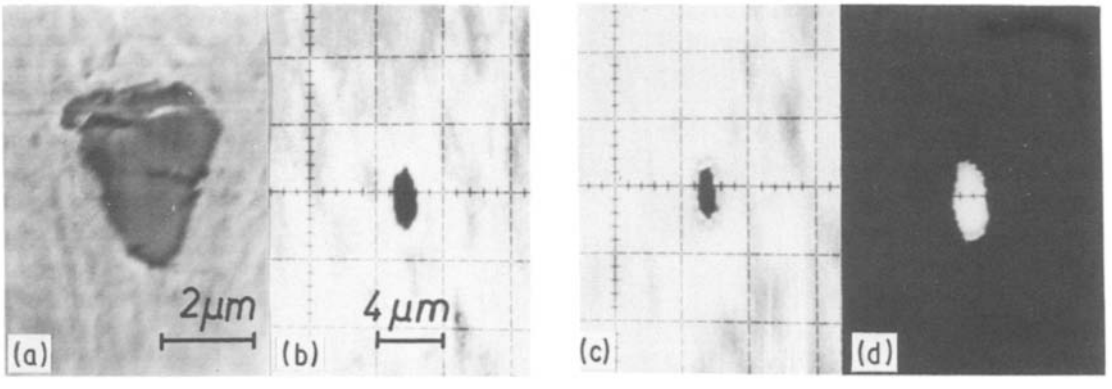

Figure 5 SEM image and appropriate SI-distributions of transparent defect and adjacent matrix. (a) SEM, (b) $^{58}Ni^+$, (c) $^{52}Cr^+$, (d) $^{27}Al^+$. (a) taken after prolonged PI-erosion, (b, c, d) after an initial period of PI-erosion.

TABLE I Types of inclusions identified in foils of different alloys

Type	Frequency of appearance	Inclusion accompanied by a hole	Matrix
Al_2O_3	o	x	NiCrAl
$(AlCr)_xO_y$	o	x	NiCr(Al-depl.)
Cr_2O_3	s	?	NiCr(Al-depl.)

phase identification of the inclusions. The following experimental parameters were selected:

Electron energy	$E(e) = 10\,keV$
Sample current	$I(sc) = 50\,nA$
Diffracting crystals	TAP, ADP

The identification procedures involved are:

(a) direct comparison of AlKα and OKα intensities of unknown and Al_2O_3-compound standard (see Fig. 6) for aluminium-rich alloys, and

(b) pure element standardization for nickel and chromium as well as compound standardization for aluminium and oxygen and subsequent data reduction by MAGIC IV-version [14] for aluminium-depleted alloys.

Owing to a pronounced reduction of particle size in the aluminium-depleted alloys a simultaneous matrix coexcitation often could not be avoided. This had to be taken into account by subtraction of a partial amount of appropriate matrix composition. The results of phase identification in foils of different alloys are gathered in Table I. The frequency of appearance is indicated by (0)-often and (s)-seldom. Those inclusions accompanied by appropriate holes and having approximately d_f-size are indicated by (x). Because they appear only seldom, the complete size

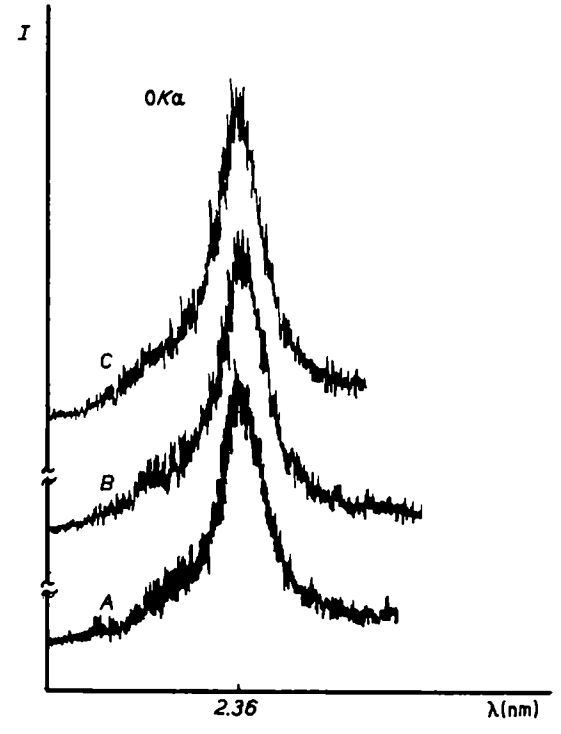

Figure 6 Comparison of O*K*α-intensities. (a) Al_2O_3-standard, (b, c) inclusions.

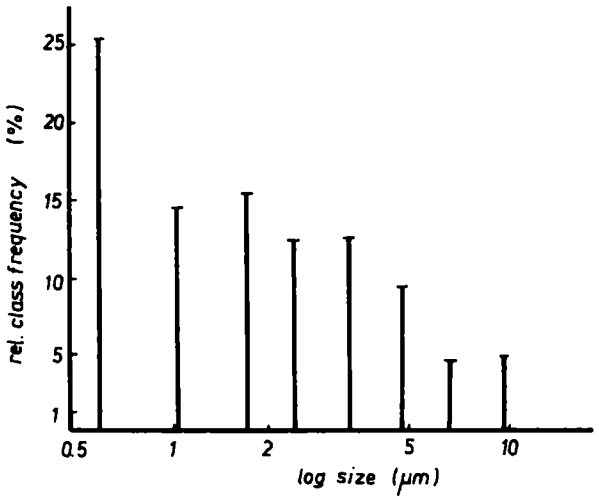

Figure 7 Size distribution of inclusions of NiCr-based alloy (ingot), QTM 720 – measurement, magnification 0.2 μm per pixel, measured content (700 $\pm$ 150) vol p.p.m., analysed area $\sim 2\,mm^2$.

distribution cannot be observed by microanalytical investigation of the foil. Therefore, the total particle distribution has been obtained from the ingot (Fig. 7) by quantitative metallography (Image Analyzer QTM 720, Cambridge Instruments). The appropriate component of second-phase particles having diameters $d_p > 3\,\mu m$ also involves those that are accompanied by foil defects.

4. Discussion

The compositions of the various types of inclusions identified are in good agreement with the qualitative thermodynamic considerations made above concerning nonmetallic second-phase formation. In particular, the formation of oxide inclusions is caused by the residual oxygen concentration in the melt and can appear instantaneously if merely an oxygen-impurity is present in the alloy. Thus this is the real reason for the formation of inclusions influencing the quality of the final foil products. According to the NiCr-alloy composition, two distinct groups of inclusions have been identified that are in close relation to the defect appearance in the foils.

1. The aluminium-rich alloy involves preferably Al_2O_3-inclusions of corundum lattice (the only stable modification under these conditions [15]. The Vickers hardness of this second phase ($H_v \sim 2000$) causes, during rolling deformation, a different mechanical behaviour compared with the ductile matrix ($H_v \sim$ 400 to 500). Therefore, if the roll gap width approaches the average d_p range it is no longer possible to avoid a considerable interaction between the Al_2O_3 inclusions and the roll surface. Owing to the lack of ductility of inclusion or inclusion/matrix interface, crack or hole formation is observed in addition to well-known effects of cavity formation [6].

2. An appropriate aluminium-depletion of the alloy does not appreciably reduce the defect formation. Instead of rather pure Al_2O_3-crystallites the formation of inclusions involving a similar lattice structure and an $(Al_{1-x}Cr_x)_2O_3$-composition is observed. Since Al_2O_3/Cr_2O_3 mixtures do not possess a miscibility gap, the real composition of the solid solution is mainly

determined by the aluminium-deficiency in the melt. Similar to α-Al_2O_3 in crystallographic structure and hardness, as well as an appropriate amount of inclusions of d_t-size, cause a quite comparable mechanical behaviour during foil finishing. In addition to the results from the aluminium-rich alloy, a chromium-depletion and thus a matrix decomposition is observed (see also [16]) in the immediate surroundings of the inclusions that will certainly result in a change of mechanical properties.

The improvement of foil quality, therefore, has to be obtained by a modification of the deoxidation procedure of the melt. The addition of, for example, rare-earth elements that form inclusions of a fine dispersion and considerably reduced hardness seems to be one way of success. From steel manufacture it is already known [13] that this procedure results in a preferred formation of rare-earth element oxides and oxysulphides. These particles exhibit an extremely reduced hardness (e.g. rare-earth sulphides $H_v \sim 450$).

Acknowledgements

The authors would like to thank their ZFW-colleagues Drs P. Müller, J. Uhlisch and M. Müller (ingot and foil preparation), Mrs E. Müller (quantitative metallography), Drs M. Bitterlich, and J. Klosowski (EPMA), Dr J. Edelmann (SEM and helpful discussions), Dr K. Friedrich (hot extraction analysis), and Dipl.-Phil. H. Fritzlar for thoroughly reading the English text version. We acknowledge the interest of Dr R. Stahlberg in this work.

References

1. A. TAYLOR and G. HINTON, *J. Inst. Metals* **81** (1952–53) 169.
2. H. GROVER and I. HUTZENLAUB, *Phys. Rev.* **56** (1939) 212.
3. C. G. SHULL and E. O. WOLLAN, *ibid.* **81** (1951) 527.
4. C. SYKES and H. EVANS, *J. Inst. Metals* **58** (1936) 255.
5. A. TAYLOR and R. W. FLOYD, *ibid.* **80** (1951/52) 577.
6. F. BARLAT, A. BARATA DA ROCHA and J. M. JALINIER, *J. Mater. Sci.* **19** (1984) 4133.
7. E. HOUDREMONT "Handbuch der Sonderstahlkunde" (Springer-Verlag, Berlin, Göttingen, Heidelberg, 1956) p. 1275.
8. H. SCHMALZRIED "Festkörperreaktionen" (Akademie-Verlag, Berlin, 1973) Chs. 7 and 8.
9. C. K. KIM and A. McLEAN, *Met. Trans.* **B10B** (1979) 585.
10. C. GRESKOVICH and V. S. STUBICAN, *J. Amer. Ceram. Soc.* **51** (1968) 42.
11. E. N. BUNTING *Bur. Stand. J. Res.* **6** (1931) 948.
12. J. F. ELLIOTT, M. GLEISER and V. RAMAKRISHNA, "Thermochemistry for Steelmaking", Vol. II. (Addison-Wesley, Reading, Mass., 1963).
13. W. G. WILSON, *Werkschrift Goldschmidt* **4** (1974) 26.
14. J. W. COLBY, *Adv. X-ray Anal.* **11** (1968) 287.
15. A. PETZOLD and W. HINZ, "Silikatchemie" (VEB Deutscher Verlag der Grundstoffindustrie, Leipzig, 1978).
16. J. H. WEBER and P. S. GILMAN, *Scripta Metall.* **18** (1984) 479.

Received 15 January
and accepted 22 May 1986